Inorg. Chem. **2003**, *42*, 4714–4723

Structural, Magnetic, and Optoelectronic Properties of (Diimine)(dithiolato)platinum(II) and -palladium(II) Complexes and Their Charge-Transfer Adducts with Nitrile Acceptors

Bradley W. Smucker,[†] Joshua M. Hudson,[‡] Mohammad A. Omary,*[,‡] and Kim R. Dunbar*[,†]

Departments of Chemistry, Texas A&M University, P.O. Box 30012, College Station, Texas 77842-3012, and University of North Texas, P.O. Box 305070, Denton, Texas 76203

Received August 19, 2002

Two new diimine dithiolato complexes, (dbbpy)Pt(dmid), **1**, and (dbbpy)Pd(dmid), **2**, were prepared and characterized (dbbpy = 4,4′-di-*tert*-butyl-2,2′-bipyridine; dmid = 2-oxo-1,3-dithiole-4,5-dithiolate). Both complexes interact with the nitrile acceptor TCNQ, and **1** also interacts with $TCNQF_4$ and TCNE (TCNQ = 7,7,8,8-tetracyanoquinodimethane; $TCNQF_4$ = 2,3,5,6-tetrafluoro-7,7,8,8-tetracyanoquinodimethane; TCNE = tetracyanoethylene) to form supramolecular 2:1 charge-transfer solids that stack in the manner –DDADDADDA– (D = electron donor; A = electron acceptor). All compounds have been fully characterized by magnetic, spectroscopic, electrochemical, and single-crystal X-ray crystallographic analyses. Magnetic susceptibility studies of the charge-transfer compounds revealed that the platinum-based complexes exhibit temperature-independent paramagnetism of $\sim 10^{-3}$ emu/mol. The donor complexes exhibit continuous absorption bands across the UV/visible and into the NIR region. Upon interaction with the nitrile acceptors, the extinction coefficients of the absorption bands increase and the energies of some d–d transitions in the NIR region change. The donor–acceptor compounds possess desired spectral features for solar cell dyes, but low conversion efficiencies resulted when a representative compound was tested in a TiO_2 solar cell. The results, however, serve to illustrate that the donor–acceptor interactions persist in solution and the adsorption of the dye molecules to the semiconductor surface occurs in the absence of typical anchoring groups. Evaluation of the spectral and electrochemical data for the title compounds and the results of the preliminary solar cell study serve as guides for future research in choosing promising candidates for efficient solar cell dyes.

Introduction

The study of charge-transfer compounds with interesting physical and spectroscopic properties has been an active area of research for over 3 decades.[1] Although purely organic charge-transfer salts exhibit interesting electronic and charge-transport properties, the incorporation of metal centers into these materials leads to d−π interactions that enhance the electronic and magnetic properties. One especially fascinating class of metal-containing charge-transfer compounds involves the complex $[Ni(dmit)_2]^{2-}$ (dmit = 2-thioxo-1,3-dithiole-4,5-dithiolate), which undergoes partial oxidation and forms superconducting salts with both open- and closed-shell organic cations.[2] A significant aspect of the solid-state interactions in these materials is the overlap of the diffuse π-orbitals on the sulfur atoms with the metal d-orbitals.[3] Additionally, depending on whether the donors and acceptors

* To whom correspondence should be addressed. E-mail: dunbar@mail.chem.tamu.edu (K.R.D.); omary@unt.edu (M.A.O.).
† Texas A&M University.
‡ University of North Texas.

(1) (a) Ferraris, J.; Cowan, D. O.; Walatka, V. V., Jr.; Perlstein, J. H. *J. Am. Chem. Soc.* **1973**, *95*, 948. (b) Coleman, L. B.; Cohen, M. J.; Sandman, D. J.; Yamagashi, F. G.; Garito, A. F.; Heeger, A. J. *J. Solid State Commun.* **1973**, *12*, 1125. (c) Wudl, F. *Acc. Chem. Res.* **1984**, *17*, 227. (d) Williams, J. M.; Ferraro, J. R.; Thorn, R. J.; Carlson, K. D.; Geiser, U.; Wang, H. H.; Kini, A. M.; Whangbo, M.-H. *Organic Superconductors (including Fullerenes)*; Prentice Hall: Englewood Cliffs, NJ, 1992.

(2) (a) Bousseau, M.; Valade, L.; Legros, J.-P.; Cassoux, P.; Garbauskas, M.; Interrante, L. V. *J. Am. Chem. Soc.* **1986**, *108*, 1908. (b) Brossard, L.; Bousseau, M.; Ribault, M.; Valade, L.; Cassoux, P. *C. R. Acad. Sci. 2* **1986**, *302*, 205. Brossard, L.; Ribault, M.; Valade, L.; Cassoux, P. *Phys. Rev. B* **1990**, *42*, 3935. (c) Cassoux, P.; Valade, L.; Kobayashi, H.; Kobayashi, A.; Clark, R. A.; Underhill, A. E. *Coord. Chem. Rev.* **1991**, *110*, 115. (d) Cassoux, P. *Coord. Chem. Rev.* **1999**, *185−186*, 213.

(3) Alvarez, S.; Vicente, R.; Hoffman, R. *J. Am. Chem. Soc.* **1985**, *107*, 6253.

10.1021/ic0259585 CCC: $25.00
Published on Web 06/21/2003

Table 1. Crystal Data for **1**−**6**

	1·CH_2Cl_2	**2**·C_6H_6	**3**·$2CH_2Cl_2$	**4**·$2CH_2Cl_2$	**5**·C_6H_6	**6**·$2CH_2Cl_2$
formula	$C_{22}H_{26}Cl_2N_2OPtS_4$	$C_{27}H_{30}N_2OPdS_4$	$C_{56}H_{56}Cl_4N_8O_2Pt_2S_8$	$C_{56}H_{52}Cl_4F_4N_8O_2Pt_2S_8$	$C_{54}H_{54}N_8O_2Pt_2S_8$	$C_{56}H_{56}Cl_4N_8O_2Pd_2S_8$
fw	728.71	633.17	1661.61	1733.58	1451.71	1484.29
space group	$P\bar{1}$	$P\bar{1}$	$P\bar{1}$	$P\bar{1}$	Cccm	$P\bar{1}$
a, Å	10.401(2)	8.1292(16)	11.200(2)	10.930(2)	11.706(2)	11.119(2)
b, Å	10.522(2)	12.834(3)	12.077(2)	12.339(3)	25.099(5)	12.086(2)
c, Å	13.214(3)	13.273(3)	12.708(3)	12.860(3)	19.033(4)	12.767(3)
α, deg	69.97(3)	84.25(3)	72.75(3)	70.96(3)	90	72.38(3)
β, deg	87.32(3)	87.86(3)	69.99(3)	69.94(3)	90	69.88(3)
γ, deg	76.68(3)	80.44(3)	78.79(3)	78.48(3)	90	78.74(3)
V, Å^3	1321.3(5)	1358.4(5)	1534.2	1531.4(6)	5592.2(19)	1527.4(5)
Z	2	2	1	1	4	1
T, K	110	110	110	110	110	110
D, g/cm^3	1.832	1.584	1.798	1.880	1.774	1.614
μ, mm^{-1}	5.847	1.014	5.049	5.072	5.345	1.086
R1[a] [$I > 4\sigma(I)$]	0.0274	0.0339	0.0504	0.0352	0.0312	0.0400
wR2[b] [$I > 4\sigma(I)$]	0.0318	0.0517	0.0947	0.0442	0.0436	0.0523
R1[a] (all data)	0.0657	0.0625	0.0848	0.0792	0.0674	0.1020
wR2[b] (all data)	0.0671	0.0665	0.0965	0.0823	0.0836	0.1095
GOF	0.996	0.913	0.833	0.984	0.998	0.758

[a] $R1 = \Sigma||F_o| - ||F_c||/|F_o|$. [b] $wR2 = \{\Sigma[w(F_o^2 - F_c^2)^2]/\Sigma[w(F_o^2)^2]\}^{1/2}$.

assemble with segregated or integrated stacks of D and A molecules in these types of charge-transfer materials, the compounds may be conductors (segregated stacks) or magnets (integrated stacks), as well-documented for a variety of both organic[4,5] and metal-containing[6,7] donor−acceptor extended-chain species. Another interesting aspect of metal-containing charge-transfer complexes is their potential use as dyes for solar cells based on wide band gap semiconductors. This technology has flourished in recent years,[8] primarily with ruthenium(II) pyridyl complexes.

One of the general goals of our research programs is to co-assemble metal complexes with organic donors and acceptors to prepare new types of molecular materials with interesting optoelectronic properties.[9,10] In the course of our studies with late transition metals, we noted literature reports that Pd(II) and Pt(II) complexes with both bpy and dmit ligands can be oxidized to form conducting materials.[11] Herein we report the syntheses of new Pd(II) and Pt(II) compounds with dbbpy and dmid and the charge-transfer products of the Pd complex with TCNQ and the Pt complex with the nitrile acceptors TCNQ, $TCNQF_4$, and TCNE. Apart from their relevance to conducting and magnetic materials, such diimine dithiolato compounds are interesting from the perspective of their electronic absorption and luminescence properties[12] and, as demonstrated by this work, their potential use as solar cell dyes for colloidal wide band gap semiconductors.

Results and Discussion

The new compounds (dbbpy)M(dmid) (M = Pd, Pt) were prepared by reacting $Na_2(dmid)$[13] with the diimine compounds (dbbpy)MCl_2. The violet compound (dbbpy)Pt(dmid), **1**, was prepared in ∼75% yield, and the wine-red species (dbbpy)Pd(dmid), **2**, was isolated in ∼60% yield. Samples of (dbbpy)M(dmid) were dissolved in CH_2Cl_2 and layered with different solutions of nitrile acceptors in a 1:1 mixture of CH_2Cl_2/C_6H_6. The resulting solutions were slowly evaporated under nitrogen to form dark blue/black crystals of [(dbbpy)M(dmid)]$_2$[A] (M = Pt, A = TCNQ, **3**; A = $TCNQF_4$, **4**; A = TCNE, **5**; M = Pd, A = TCNQ, **6**). The 2:1 D:A ratio in the products was observed to form even when a 1:1 ratio of the starting materials was employed.

X-ray Crystallographic Studies. Crystal data for compounds **1**−**6** are listed in Table 1. X-ray-quality crystals of **1**·CH_2Cl_2 and **2**·C_6H_6 were grown by slow evaporation of dichloromethane and dichloromethane/benzene solutions of the compounds, respectively. Figure 1 shows the molecular structure of **1**. The palladium analogue, **2**, exhibits the same square planar geometry as that in **1**. In both **1**·CH_2Cl_2 and

(4) (a) Shaik, S. S. *J. Am. Chem. Soc.* **1982**, *104*, 5328. (b) McConnell, H. M.; Hoffman, B. M.; Metzger, R. M. *Proc. Natl. Acad. Sci. U.S.A.* **1965**, *53*, 46.

(5) Miller, J. S.; Epstein, A. J. *J. Am. Chem. Soc.* **1987**, *109*, 3850.

(6) (a) Cassoux, P.; Valade, L. In *Inorganic Materials*, 2nd ed.; Bruce, D. W., O'Hare, D., Eds.; John Wiley & Sons: Chichester, U.K., 1996. (b) Tanaka, H.; Okano, Y.; Kobayashi, H.; Suzuki, W.; Kobayashi, A. *Science* **2001**, *291*, 285. (c) Bigoli, F.; Deplano, P.; Mercuri, M. L.; Pellinghelli, M. A.; Pilia, L.; Pintus, G.; Serpe, A.; Trogu, E. F. *Inorg. Chem.* **2002**, *41*, 5241.

(7) (a) Coomber, A. T.; Beljonne, D.; Friend, R. H.; Brédas, J. K.; Charlton, A.; Robertson, N.; Underhill, A. E.; Kurmoo, M.; Day, P. *Nature* **1996**, *380*, 144. (b) Robertson, N.; Cronin, L. *Coord. Chem. Rev.* **2002**, *227*, 93.

(8) For a review on the topic, see: Kalyanasundaram, K.; Grätzel, M. Efficient Photovoltaic Solar Cells Based on Dye Sensitization of Nanocrystalline Oxide Films. In *Optoelectronic Properties of Inorganic Compounds*; Roundhill, D. M., Fackler, J. P., Jr., Eds.; Plenum Press: New York, 1999; Chapter 5.

(9) (a) Smucker, B. W.; Dunbar, K. R. *Dalton Trans.* **2000**, *8*, 1309. (b) Miyasaka, H.; Campos-Fernández, C. S.; Clérac, R.; Dunbar, K. R. *Angew. Chem., Int. Ed.* **2000**, *39*, 3831. (c) Zhao, H.; Heintz, R. A.; Ouyang, X.; Dunbar, K. R. *Chem. Mater.* **1999**, *11*, 736. (d) Fourmigué, M.; Uzelmeier, C. E.; Boubekeur, K.; Bartley, S. L.; Dunbar, K. R. *J. Organomet. Chem.* **1997**, *529*, 343.

(10) (a) Omary, M. A.; Kassab, R. M.; Haneline, M. R.; Bjeirami, O. E.; Gabbaï, F. P. *Inorg. Chem.* **2003**, *42*, 2176. (b) Rawashdeh-Omary, M. A.; Omary, M. A.; Fackler, J. P., Jr.; Galassi, R.; Pietroni, B. R.; Burini, A. *J. Am. Chem. Soc.* **2001**, *123*, 9689.

(11) Vicente, R.; Ribas, J.; Cassoux, P.; Sourisseau, C. *Synth. Met.* **1986**, *15*, 79.

(12) (a) Zuleta, J. A.; Chesta, C. A.; Eisenberg, R. *J. Am. Chem Soc.* **1989**, *111*, 8916. (b) Zuleta, J. A.; Bevilacqua, J. M.; Proserpio, D. M.; Harvey, P. D.; Eisenberg, R. *Inorg. Chem.* **1992**, *31*, 2396. (c) Cummings, S. D.; Eisenberg, R. *J. Am. Chem. Soc.* **1996**, *118*, 1949. (d) Paw, W.; Cummings, S. D.; Mansour, M. A.; Connick, W. B.; Geiger, D. K.; Eisenberg, R. *Coord. Chem. Rev.* **1998**, *171*, 125.

(13) Fourmigué, M.; Lenoir, C.; Coulon, C.; Guyon, F.; Amaudrut, J. *Inorg. Chem.* **1995**, *34*, 4979.

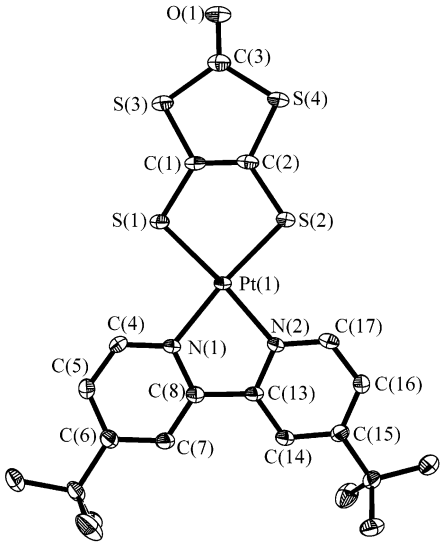

Figure 1. Thermal ellipsoid plot at the 50% probability level, showing the molecular structure of (dbbpy)Pt(dmid), **1**. The dichloromethane solvent molecule and hydrogen atoms are omitted for the sake of clarity.

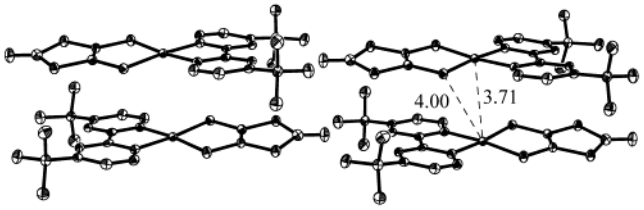

Figure 2. Thermal ellipsoid plot at the 50% level showing the head-to-tail molecular packing and the intermolecular Pd···Pd and Pd···S distances (in Å) in (dbbpy)Pd(dmid), **2**. The benzene solvent molecules and hydrogen atoms are omitted for the sake of clarity.

2·C_6H_6, the individual molecules are stacked in a head-to-tail arrangement (the representative Pd molecules are shown in Figure 2). For **1**·CH_2Cl_2, the platinum molecules are positioned such that the metal center of one molecule is situated directly above a bridging carbon on the bipyridine ring of an adjacent molecule. The intermolecular distances between the stacks of **1**·CH_2Cl_2 are >3.65 Å. In **2**·C_6H_6, the metal centers are nearly in registry with Pd···Pd distances of ∼3.71 Å and Pd···S distances of ∼4.0 Å.

In all of the molecular structures of compounds **3**−**6**, the metal diimine dithiolato donors and nitrile acceptors assemble in a 2:1 ratio and stack in the manner (−DDADDADDA−). As a representative example, Figure 3 shows this stacking pattern for **3**·$2CH_2Cl_2$. The distances between adjacent molecules in **3**−**6** are in the range 3.2−3.6 Å and are shorter than the D−D distances in the parent compounds **1** and **2** (∼3.7 Å; Table 2). The distances between the donor and acceptor molecules are well within the range of π-interactions[1] and are similar to the intermolecular distances between partially oxidized molecules of tetrathiafulvalene (TTF), which is an indication of some degree of charge transfer. A similar situation was encountered previously by Fackler and co-workers for trinuclear Au(I) compounds, which also form −DDADDADDA− stacks with TCNQ in which shorter D−D distances were observed and attributed to partial oxidation of the metal center.[10b] As in the packing of compounds **1** and **2**, the crystal structures of compounds

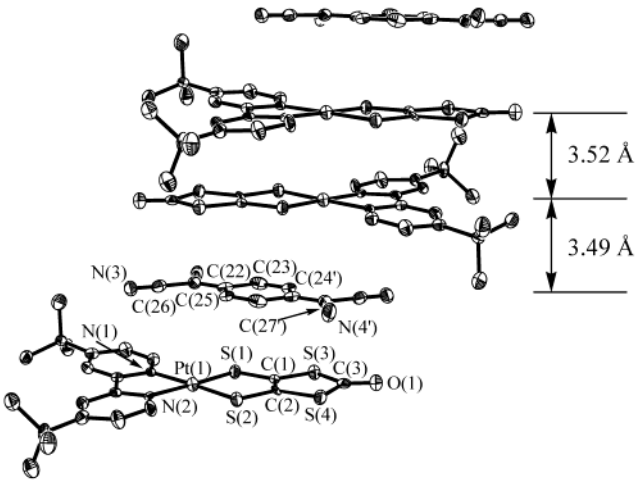

Figure 3. Thermal ellipsoid plot at the 50% level showing the stacking in [(dbbpy)Pt(dmid)]$_2$[TCNQ], **3**, with the donor−donor and donor−acceptor distances noted. The dichloromethane solvent molecules and hydrogen atoms are omitted for the sake of clarity.

Table 2. Intermolecular Distances Representing Donor−Donor and Donor−Acceptor Interactions in **1**−**6**[a]

compd	d_{D-A}, Å	d_{D-D}, Å	d_{M-M}, Å
(dbbpy)Pt(dmid) (**1**)		3.66	4.88
(dbbpy)Pd(dmid) (**2**)		3.59	3.71
[(dbbpy)Pt(dmid)]$_2$[TCNQ] (**3**)	3.49	3.52	3.74
[(dbbpy)Pt(dmid)]$_2$[$TCNQF_4$] (**4**)	3.36	3.46	3.77
[(dbbpy)Pt(dmid)]$_2$[TCNE] (**5**)	3.21	3.58	5.00
[(dbbpy)Pd(dmid)]$_2$[TCNQ] (**6**)	3.42	3.47	3.72

[a] Notation: d_{X-Y}, distance between X and Y; D = plane of the donor Pt or Pd compound; A = plane of the nitrile acceptor compound; M = metal atom.

3−**6** are such that the individual donor molecules are stacked in a head-to-tail arrangement.

For **3**·$2CH_2Cl_2$, the shortest contact between the planes of the (dbbpy)Pt(dmid) and TCNQ molecules is 3.49 Å and the shortest distance between the Pt donor molecules is 3.52 Å. The intermolecular Pt···Pt distance in **3**·$2CH_2Cl_2$ is 3.74 Å with the shortest intermolecular Pt−S distance being 3.77 Å. The TCNQ molecule in the charge-transfer adduct **3**·$2CH_2Cl_2$ exhibits C≡N bond lengths of 1.123(9) and 1.111(10) Å. The exocyclic C═C bond length is 1.367(10) Å, and the quinone C═C distance is 1.323(10) Å. Other significant bond distances and angles are compiled in Table 3.

Compound **4**·$2CH_2Cl_2$ with the $TCNQF_4$ acceptor also crystallizes in the $P\bar{1}$ space group with the same donor−acceptor stacking as that found in the TCNQ adduct, **3**. The shortest distance between the planes of the donor and acceptor is 3.36 Å while the distance between the two donors is 3.46 Å. The $TCNQF_4$ molecule is situated between the (dbbpy)Pt(dmid) molecules in such a way that one of the F atoms is positioned almost directly above the Pt atom with an intermolecular Pt···F separation of 3.45 Å. The intermolecular Pt···Pt distance is 3.77 Å, and the closest intermolecular Pt···S distance is 3.66 Å. The exocyclic C═C bond length is 1.393(9) Å, which is longer than the corresponding distance of 1.372 Å in neutral $TCNQF_4$[14] but shorter than the distance found in the $TCNQF_4^{\bullet-}$ radical anion (1.435 Å).[15] This intermediate distance is indicative

Table 3. Selected Bond Distances (Å) and Angles (deg) for **1**−**6** with Standard Deviations in Parentheses

				1			
Pt1−N1	2.052(3)	S1−C1	1.748(4)	S3−C3	1.770(4)	N1−C8	1.361(4)
Pt1−N2	2.050(3)	S2−C2	1.746(4)	S4−C3	1.768(4)	C4−C5	1.389(5)
Pt1−S1	2.2623(12)	S3−C1	1.746(4)	C1−C2	1.340(6)		
Pt1−S2	2.2667(13)	S4−C2	1.750(4)	N1−C4	1.342(5)		
N2−Pt1−N1	79.58(12)	C1−S1−Pt1	102.14(14)	S3−C1−S1	120.4(2)	N1−C8−C13	114.4(3)
N2−Pt1−S1	173.62(9)	C2−C1−S1	122.5(3)	S4−C3−S3	113.0(2)		
N2−Pt1−S2	94.44(9)	C1−S3−C3	96.28(19)	N1−C4−C5	122.6(3)		
				2			
Pd1−N1	2.051(2)	S1−C1	1.745(3)	S3−C3	1.779(3)	N1−C8	1.358(3)
Pd1−N2	2.054(2)	S2−C2	1.742(3)	S4−C3	1.782(3)	C4−C5	1.370(4)
Pd1−S1	2.2675(11)	S3−C1	1.751(3)	C1−C2	1.347(4)		
Pd1−S2	2.2636(10)	S4−C2	1.741(3)	N1−C4	1.341(3)		
N2−Pd1−N1	78.88(9)	C1−S1−Pd1	102.26(9)	S3−C1−S1	120.33(16)	N1−C8−C9	114.2(2)
N2−Pd1−S1	173.14(6)	C2−C1−S1	122.8(2)	S4−C3−S3	111.70(15)		
N2−Pd1−S2	94.99(7)	C1−S3−C3	96.92(13)	N1−C4−C5	122.7(3)		
				3			
Pt1−N1	2.059(6)	S2−C2	1.735(8)	C1−C2	1.320(10)	C24−C23	1.323(10)
Pt1−N2	2.066(6)	S3−C1	1.759(8)	N1−C4	1.309(9)	C26−N3	1.123(9)
Pt1−S1	2.261(2)	S4−C2	1.750(7)	N1−C8	1.375(9)	C27−N4	1.111(10)
Pt1−S2	2.266(2)	S3−C3	1.781(8)	C4−C5	1.373(10)		
S1−C1	1.750(7)	S4−C3	1.769(8)	C22−C25	1.367(10)		
N1−Pt1−N2	80.6(2)	C1−S1−Pt1	101.7(3)	S3−C1−S1	119.5(5)	N1−C8−C9	116.1(6)
N2−Pt1−S1	174.42(18)	C2−C1−S1	123.0(6)	S4−C3−S3	111.8(4)	C26−C25−C27	115.9(7)
N2−Pt1−S2	95.15(17)	C1−S3−C3	96.3(4)	N1−C4−C5	122.3(7)	C23−C22−C25	121.5(7)
				4			
Pt1−N1	2.025(6)	S2−C2	1.748(6)	C1−C2	1.352(10)	C44−C45	1.335(10)
Pt1−N2	2.040(6)	S3−C1	1.728(7)	N1−C4	1.352(9)	C50−N5	1.150(9)
Pt1−S1	2.2692(19)	S4−C2	1.721(7)	N1−C8	1.366(8)	C51−N6	1.134(9)
Pt1−S2	2.257(2)	S3−C3	1.765(7)	C4−C5	1.373(10)	C44−F1	1.334(8)
S1−C1	1.738(7)	S4−C3	1.826(7)	C43−C49	1.393(9)	C45−F2	1.341(7)
N1−Pt1−N2	80.0(2)	C1−S1−Pt1	102.7(3)	S3−C1−S1	120.3(5)	N1−C8−C9	114.2(6)
N2−Pt1−S1	173.46(16)	C2−C1−S1	121.9(5)	S4−C3−S3	110.5(3)	C50−C49−C51	112.4(7)
N2−Pt1−S2	93.59(16)	C1−S3−C3	97.5(3)	N1−C4−C5	122.2(6)	C45−C43−C44	113.5(7)
				5			
Pt1−N1	2.032(4)	S2−C1	1.742(4)	N1−C3	1.350(6)	C12−C12	1.341(14)
Pt1−S1	2.2533(11)	S2−C2	1.773(4)	N1−C7	1.363(5)	C13−N2	1.139(7)
S1−C1	1.735(4)	C1−C1	1.344(9)	C3−C4	1.362(6)		
N1−Pt1−N1	79.3(2)	C1−C1−S1	122.30(15)	S2−C2−S2	112.3(4)	C13−C12−C12	121.6(7)
N1−Pt1−S1	174.46(10)	C1−S2−C2	96.4(2)	N1−C3−C4	123.1(4)		
N1−Pt1−S1	95.14(11)	S2−C1−S1	120.2(3)	C13−C12−C13	116.3(7)		
				6			
Pd1−N1	2.060(4)	S2−C2	1.733(5)	C1−C2	1.335(7)	C44−C45	1.320(8)
Pd1−N2	2.051(4)	S3−C1	1.746(5)	N1−C4	1.325(6)	C50−N5	1.140(7)
Pd1−S1	2.2548(16)	S4−C2	1.755(5)	N1−C8	1.359(6)	C51−N6	1.145(7)
Pd1−S2	2.2719(14)	S3−C3	1.774(5)	C4−C5	1.383(7)		
S1−C1	1.741(5)	S4−C3	1.783(5)	C43−C49	1.356(7)	N1−C8−C9	115.7(4)
N1−Pd1−N2	79.58(15)	C1−S1−Pd1	102.04(18)	S3−C1−S1	120.4(3)	C50−C49−C51	114.8(5)
N2−Pd1−S1	173.55(10)	C2−C1−S1	122.7(4)	S4−C3−S3	111.5(3)	C49−C43−C44	122.0(5)
N2−Pd1−S2	95.90(11)	C1−S3−C3	97.4(2)	N1−C4−C5	122.7(5)		

of a degree of charge transfer, as in the case of the TCNQ adduct **3**. Other significant distances are exhibited in Table 3.

In a manner akin to the other D_2A compounds in this series, the TCNE acceptor in **5**·C_6H_6 is sandwiched between two (dbbpy)Pt(dmid) donors (Figure 4). The donors are, as in the other compounds, packed in a head-to-tail fashion with the bipyridine rings located above each other. The distance between the planes of the two donor molecules is 3.58 Å, and the shortest distance between the TCNE acceptor and the donor is 3.21 Å. In the structure of compound **5**, the TCNE molecule exhibits a C≡N bond length of 1.139(7) Å and the ethylene C═C bond length is 1.341(14) Å. The TCNE molecule is slightly canted such that each ethylene carbon is orientated toward the Pt atom in (dbbpy)Pt(dmid). Whereas adducts of the other nitrile acceptors of this type form sheets composed of planar donor or acceptor molecules arranged in columns of −DDADDADDA− in the $P\bar{1}$ space group, the TCNE derivative crystallizes in the higher symmetry space group *Cccm* with the stacks of −DDADDADDA− forming two distinct sheets. These separate sheets are oriented in such a way that the individual molecules of one sheet are aligned at an angle of 54.3° with respect to molecules in adjacent sheets (Figure 4).

The crystal structure of **6**·$2CH_2Cl_2$ revealed that the compound is isostructural with **3**·$2CH_2Cl_2$. The distances between the stacks are very similar to those in **3**, with the

(14) Emge, T. J.; Maxfield, M.; Cowan, D. O.; Kistenmacher, T. J. *Mol. Cryst. Liq. Cryst.* **1981**, *65*, 161.
(15) Miller, J. S.; Zhang, J. H.; Reiff, W. M. *Inorg. Chem.* **1987**, *26*, 600.

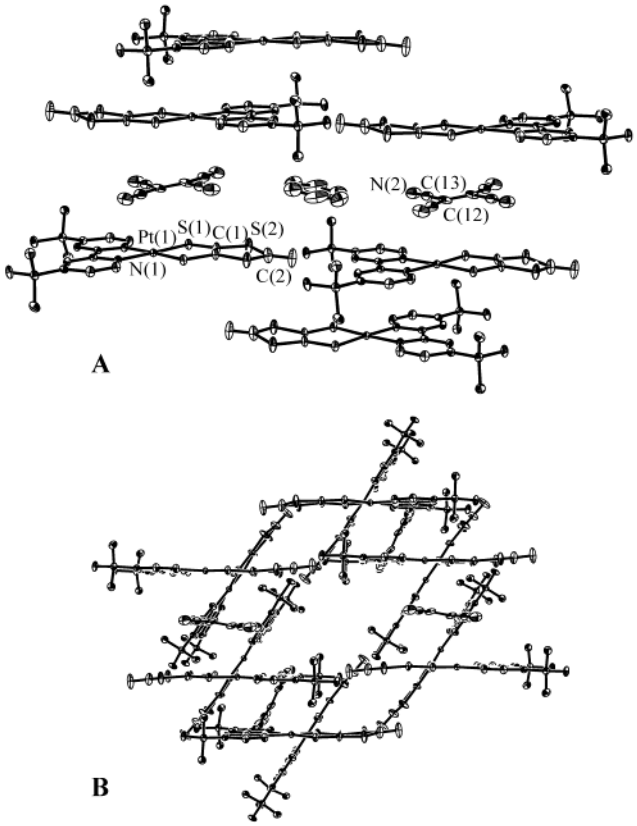

Figure 4. (A) A 50% thermal ellipsoid representation of [(dbbpy)Pt(dmid)]$_2$[TCNE], **5**, with hydrogen atoms omitted and only one orientation of a distorted benzene molecule shown for the sake of clarity. The interstitial benzene occupies the space between the TCNE molecules. (B) Two sheets of −DDADDADDA− shown with the foreground sheet being horizontal and the background being orientated at an angle of 54.3° from the foreground sheet.

shortest D−D and D−A contacts being 3.47 and 3.42 Å, respectively. These distances are significantly shorter than the D−D distances in the parent compound **2** (∼3.7 Å).

The fact that the TCNQ adducts **3** and **6** adopt the same packing arrangement, irrespective of the metal, underscores the importance of the favorable interactions between the donor and acceptor. Additionally, the similar stacking motif (−DDADDADDA−) of all the donor−acceptor adducts **3**−**6** is a significant indication of the energy stabilization that results from the interactions between the molecules in these supramolecular stacks.

Magnetic Susceptibility and Conductivity Measurements. Magnetic studies of crystals of compounds **3**−**5** revealed temperature-independent paramagnetism, TIP (χ_{TIP} = 2 × 10^{-3}, 2 × 10^{-3}, and 1 × 10^{-3} emu/mol for **3**−**5**, respectively), representing 1 order of magnitude higher than typical TIP susceptibilities.[16] The appreciable χ_{TIP} values hinted that Pauli paramagnetism associated with conduction electrons may be responsible for these values, but the conductivities of pressed pellets of **3** are very low (∼10^{-6} Ω^{-1} cm^{-1} at 300 K). In contrast, compound **6** is diamagnetic, which indicates that this complex does not have the same conducting behavior as compounds **3**−**5**. Scanning electron microscopy (SEM) was used to qualitatively characterize the conductivity of the donor−acceptor compounds **3**−**6**. SEM images are shown in Figure 5 for crystals of **3**−**6**. The observation of clear SEM images for crystals that were not coated with a conducting film suggests that these crystals are noninsulators. The charge from the electron beam accumulates on the surface of insulating materials, which leads to bright spots that preclude the observation of clear SEM images for insulators.[17] On the other hand, if the charge is diffused within conducting or semiconducting materials, SEM images that clearly show the details of the surface are observed. The fact that a less clear image was obtained for the Pd compound **6** than the images for the Pt analogues suggests that crystals of **6** are qualitatively less conductive than those of the Pt compounds. Because of the small size and shape and the instability of the crystals due to solvent loss, two- and four-probe single-crystal conductivity measurements on compounds **3**−**6** could not be reliably performed.

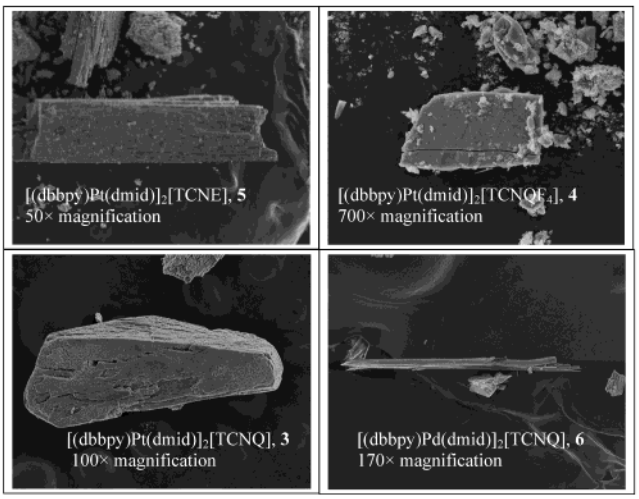

Figure 5. SEM images of [(dbbpy)M(dmid)]$_2$[TCNX] crystals.

Cyclic Voltammetric and Infrared Studies. Cyclic voltammetric studies of **1** and **2** revealed two reversible oxidations located at $E_{1/2}$ = +1.44 and +0.55 V and one reversible reduction at $E_{1/2}$ = −1.32 V for **1** and two reversible oxidations at $E_{1/2}$ = +1.48 and +0.64 V and one irreversible reduction at E_{pc} = −1.42 V for **2**. The reductions are assigned to the dbbpy ligand, and the oxidations are attributed to the M−dmid unit.[12b,13] The reversible oxidation processes and the magnitudes of the positive oxidation potentials suggest that **1** and **2** are good electron donors. This was the rationale for reacting these electron donor complexes with the organic electron acceptors. The goal is to form donor−acceptor charge-transfer complexes, in a manner akin to reactions of chalcogen-based organic donor molecules such as tetrathiafulvalene (TTF) with TCNQ.[1a,b] In dichloromethane solutions, compounds **3**−**6** exhibit an electrochemical behavior that is similar to that of the starting

(16) Carlin, R. L. *Magnetochemistry*; Springer-Verlag: Berlin, 1986.

(17) Goldstein, J. I.; Newbury, D. E.; Echlin, P.; Joy, D. C.; Romig, A. D., Jr.; Lyman, C. E.; Fiori, C.; Lifshin, E. *Scanning Electron Microscopy and X-ray Microanalysis: A Text for Biologists, Materials Scientists, and Geologists*; Plenum Press: New York, 1992.

Table 4. Cyclic Voltammetric Data for Compounds **1**−**6**[a]

compd	$E_{1/2}$(ox), donor	$E_{1/2}$(red), donor	$E_{1/2}$(red), acceptor
(dbbpy)Pt(dmid) (**1**)	0.55	−1.32	
	1.44		
(dbbpy)Pd(dmid) (**2**)	0.64	−1.42	
	1.48		
[(dbbpy)Pt(dmid)]$_2$[TCNQ] (**3**)	0.54	−1.30	0.19
	1.41		−0.33
[(dbbpy)Pt(dmid)]$_2$[TCNQF$_4$] (**4**)	0.59	−1.37	0.59
	1.48		0.00
[(dbbpy)Pt(dmid)]$_2$[TCNE] (**5**)	0.48	−1.42	0.17
	1.35		−0.84
[(dbbpy)Pd(dmid)]$_2$[TCNQ] (**6**)	0.64	−1.48	0.15
	1.46		−0.40

[a] Values listed are volts vs Ag/AgCl, Pt disk electrode in 0.1 M [*n*-Bu$_4$N][PF$_6$]/CH$_2$Cl$_2$ at a scan rate of 100 mV/s.

materials, namely (dbbpy)M(dmid) and the corresponding acceptor (Table 4). Because the electrochemical measurements for compounds **3**−**6** were carried out in solution, the packing arrangement observed in the crystals no longer exists. The electronic properties discussed below, however, indicate some pairing between the acceptor and donor in solution even though this pairing was not detected electrochemically.

The extent of charge transfer in compounds of the acceptor TCNQ has been the subject of numerous IR and Raman spectroscopic studies.[18] A compilation of ν(C≡N) stretching modes for a large number of TCNQ compounds allows for a useful empirical correlation between the frequency of the ν(C≡N) mode and extent of charge transfer.[19] The ν(C≡N) stretches for the Pt and Pd adducts of TCNQ described here (**3** and **6**) correspond to a partial charge of $\rho \sim -0.4$ on the TCNQ units. In addition, there are noticeable shifts in the δ(C−H) out-of-plane bending vibrational frequencies between the (dbbpy)M(dmid) starting materials (824 and 828 cm^{-1} in **1** and **2**, respectively) and their respective nitrile adducts (832, 834, 839, and 835 cm^{-1} for **3**−**6**, respectively). These shifts are also indicative of the corresponding partially oxidized (dbbpy)M(dmid) species and are in accordance with the intermediate crystallographic distances between the neutral and fully reduced nitriles (vide supra).

Electronic Properties and Potential Use in Solar Cells. In light of the interest in the photophysical properties of similar systems,[12] the electronic properties of the title compounds were also investigated. Figures 6 and 7 illustrate the solution absorption spectra and the solid-state diffuse reflectance spectra, respectively, for the TCNQ adducts and the parent compounds while similar spectra involving other nitrile adducts are available in the Supporting Information.

Figure 6 depicts the electronic absorption spectrum of [(dbbpy)Pt(dmid)]$_2$[TCNQ], **3**, and the parent compound (dbbpy)Pt(dmid), **1**, in CH$_2$Cl$_2$ solutions. A significant increase in molar absorptivity is observed with the introduction of the organic acceptor for all complexes in general, as illustrated by the representative example shown in Figure 6 (see the Supporting Information for other compounds). The strong absorption bands labeled "a" and "c", respectively, are diimine $\pi-\pi^*$ and charge transfer to diimine from either a dithiolate or a metal-filled d orbital, according to literature assignments of similar Pt(II) diimine dithiolato complexes.[12,20] The absorption bands labeled "b" with maxima near 400 and 850 nm for **3** are absent in solutions of **1** but observed for free TCNQ and, therefore, they are assigned to TCNQ-centered $\pi-\pi^*$ transitions. The low energy and comparatively low extinction coefficients for the other absorption peaks in the NIR region (labeled "d") are consistent with an assignment to d−d transitions from the various filled 5d orbitals to the vacant 5d$_{x^2-y^2}$ orbital of Pt(II). The NIR absorptions due to d−d transitions clearly distinguish the donor−acceptor adduct **3** in solution from the parent molecules **1** and free TCNQ. One could be misled to conclude that the weak donor−acceptor interactions observed in the solid stacks dissociate in solution if the conclusion was based on absorption measurements using typical UV/visible spectrophotometers that do not access the NIR region. The presence of the organic acceptor molecule alters the Pt(II) environment in **1** and perturbs the electronic structure, since the geometry is altered owing to the weak interaction with TCNQ. Hence, the energies of some d−d transitions are affected as observed in the NIR spectra. This is selective for certain d−d bands (see dashed lines in Figure 6) because the interaction with TCNQ is direction specific as shown in the crystallographic data. The increased extinction coefficient upon interaction with acceptors is likely due to the reduced symmetry in the adducts compared to the donor molecules. One notices from Table 3 that the M−N1 and M−N2 distances are essentially the same in the donor complexes alone while they become significantly different in the corresponding adducts with TCNQ. The same argument is valid for the M−S1 and M−S2 distances. If these trends persist in solution, it is not unreasonable to argue that the site symmetry of the complex is reduced from C_{2v} in the donor molecules **1** and **2** to C_s in the adducts **3** and **6** (or even C_1 if one considers the weak interaction with TCNQ).

Figure 7 depicts the diffuse reflectance spectra for solids of the TCNQ adducts compared to the free donors of the Pt (bottom) and Pd (top) compounds. The solid-state data in general are similar to the solution data described above with some minor differences that are not surprising in view of the differences between solids and solutions in terms of the presence and absence of solvation and packing effects. For example, extra diimine $\pi-\pi^*$ bands appear for the solids at short wavelengths (e.g., ∼235 nm) due to the absence of CH$_2$Cl$_2$, whose strong absorption in this region precludes the appearance of these bands in solution. The increased resolution in the solid state for some bands (e.g., the charge-transfer bands "c") is also due to the absence of solvent since interaction with solvent molecules is known to cause band broadening. The slight energy shifts for some bands on going

(18) (a) Pukacki, W.; Pawlak, M.; Graja, A.; Lequan, M.; Lequan, R. M. *Inorg. Chem.* **1987**, *26*, 1328. (b) Bozio, R.; Gerlando, A.; Pecile, C. *J. Chem. Soc., Faraday. Trans. 2* **1975**, *71*, 1237. (c) Bozio, R.; Zanon, I.; Girlando, A.; Pecile, C. *J. Chem. Soc., Faraday Trans. 2* **1978**, *74*, 235.

(19) Chappell, J. S.; Bloch, A. N.; Bryden, W. A.; Maxfield, M.; Poehler, T. O.; Cowan, D. O. *J. Am. Chem. Soc.* **1981**, *103*, 2442.

(20) For a review, see: Fleeman, W. L.; Connick, W. B. *Comments Inorg. Chem.* **2002**, *23*, 205.

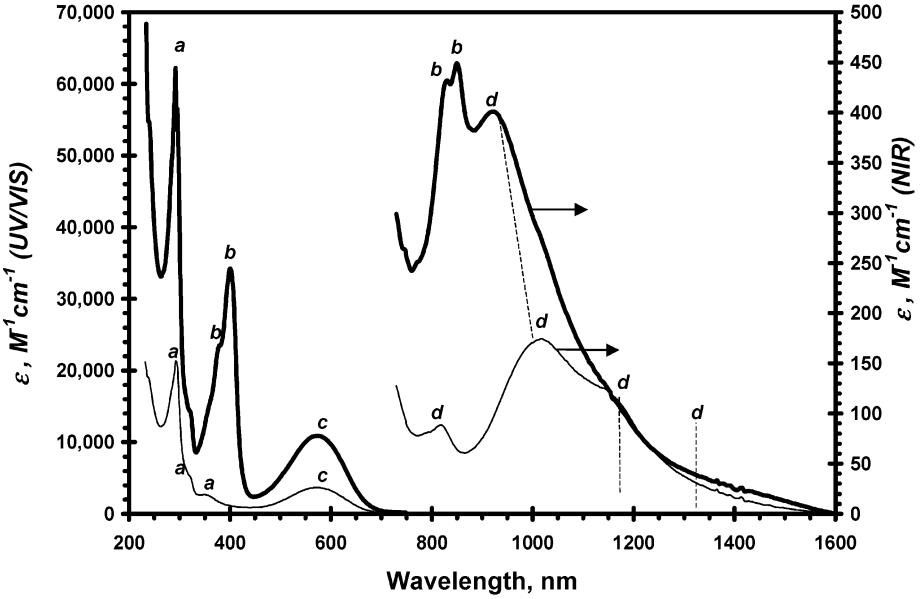

Figure 6. Electronic absorption spectra for dichloromethane solutions of (dbbpy)Pt(dmid), **1** (thin line), and [(dbbpy)Pt(dmid)]$_2$[TCNQ], **3** (thick line), in the UV/vis region (left) and NIR region (right). Assignment notation: a, $\pi-\pi^*$ (diimine); b, $\pi-\pi^*$ (TCNQ); c, charge transfer to diimine; d, d−d transitions.

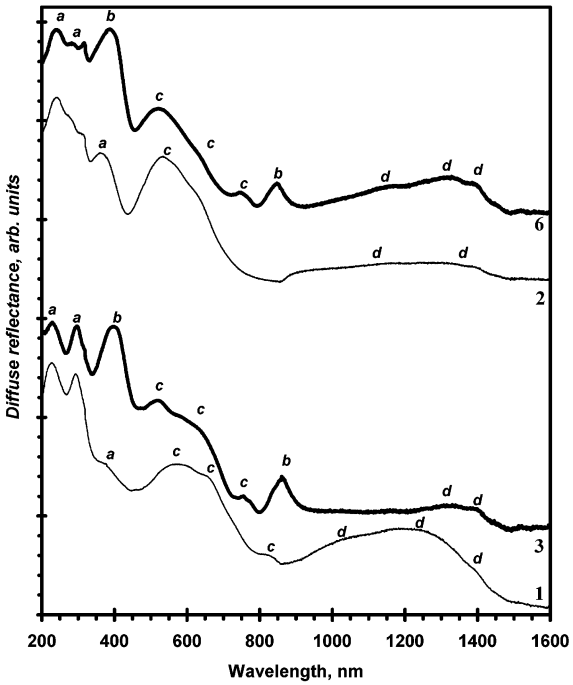

Figure 7. Diffuse reflectance spectra for solids of (dbbpy)Pt(dmid), **1**, [(dbbpy)Pt(dmid)]$_2$[TCNQ], **3**, (dbbpy)Pd(dmid), **2**, and [(dbbpy)Pd(dmid)]$_2$-[TCNQ], **6**. Assignment notation: a, $\pi-\pi^*$ (diimine); b, $\pi-\pi^*$ (TCNQ); c, charge transfer to diimine; d, d−d transitions. The arbitrary intensities are adjusted and offset for the sake of clarity.

from the solution to the solid state are not surprising in view of the packing effects and absence of solvent interactions in the solid state. The better resolution of the diffuse reflectance spectra for the solids compared to the solution absorption spectra allows for a clearer illustration of the donor−acceptor interactions as the energies and number of charge transfer and d−d bands for adducts **3** and **6** are clearly different from those in the parent donor compounds **1** and **2** (Figure 7). The similarity of the electronic structure between the Pt and Pd compounds is evident in Figure 7, which is consistent with the similarity in the crystal structures of the analogous Pt and Pd compounds. Hence, only one compound (the Pt compound, **3**) was used for the preliminary solar cell investigation described below. The observations, and the corresponding spectral assignments regarding Figures 6 and 7, are generally valid for the remaining compounds. The spectral properties of all the compounds are deposited in the Supporting Information.

The absorption and diffuse reflectance spectra for solutions and solids of **3**−**6** reveal a conspicuous absence of discernible bands that may be reasonably assigned to charge transfer from the donor complex to the nitrile acceptor. An inspection of Figures 6 and 7 reveals that the charge-transfer bands "c" for the donor−acceptor adducts are similar to those of the isolated donor compounds with no additional lower energy bands or broadening of bands "c" toward the red region. These results appear to contradict the aforementioned crystallographic, infrared, and magnetic susceptibility results, which clearly imply the presence of donor−acceptor interactions in the adducts (vide supra). The explanation lies in the stacking pattern of adducts **3**−**6**. Kisch and co-workers have established that donor-to-acceptor charge transfer absorption bands are observed only in 1:1 but not 2:1 donor−acceptor adducts.[21]

Given that similar diimine dithiolato complexes of Pt(II) were reported to be luminescent,[12] we have attempted to carry out luminescence studies for the title compounds. No luminescence was observed, however, for the title compounds even at cryogenic temperatures for solids and solutions. This is likely to be a consequence of the expected low luminescence energy in the NIR region, which would be the case in the presence of a significant Stokes' shift. Luminescence in the NIR region is inaccessible by our (and most commercial)

(21) (a) Kisch, H.; Eisen, B.; Dinnebier, R.; Shankland, K.; David, W. I. F.; Knoch, F. *Chem.—Eur. J.* **2001**, *7*, 738. (b) Kisch, H. *Comments Inorg. Chem.* **1994**, *16*, 113.

spectrofluorometers. Moreover, such a low-energy luminescence is particularly prone to nonradiative multiphonon relaxation processes to the ground state, the rates of which increase when the gap separating the excited state from the ground state decreases, as dictated by the energy gap law.[22] It is also worthwhile noting that photophysical kinetic studies for Pt(II) diimine dithiolato complexes have suggested that the presence of low-lying metal-centered d−d states contributes to the quenching mechanism of such complexes.[12c,20] Therefore, the very low energies of the d−d transitions for the compounds in this study (in the NIR region as illustrated in Figures 6 and 7) are expected to be partially responsible for the absence of luminescence.

The continuous strong absorption for **3** across the visible and into the NIR region prompted us to probe its action as a dye for solar cells with wide band gap semiconductors such as TiO_2 and SnO_2. The most important finding thus far is the ability of **3** to adsorb onto the surface of TiO_2, despite the absence of typical anchoring groups such as carboxylates or phosphonates in the aromatic diimine ligands. Molecules of **1**, for example, are not capable of adsorption onto TiO_2 surfaces by themselves due to the absence of such anchoring groups.

The details of the solar cell experiment using standard 8 + 3 μm-thick TiO_2 electrodes have been described previously.[23] The TiO_2 electrodes were first heated to 450 °C for 20 min and allowed to cool to ∼40 °C, and then the electrodes were plunged into the blue dye solution, a 6.0×10^{-4} M dichloromethane solution of **3**. After 3 h, the electrodes became highly colored with the intense blue color of the dye. The spectral response of the resulting electrodes was very similar to the solution spectra. The significance of this result encompasses both practical and fundamental aspects. In terms of applied research, this result opens up a new avenue for the development of new solar cell dyes that do not require typical anchoring groups such carboxylates, sulfonates, and phosphonates on the diimine. From a fundamental chemical standpoint in support of the themes of this paper, the adsorption of the dye onto the semiconductor surface from a dilute solution of **3** supports the conclusion that the donor−acceptor interaction between (dbbpy)Pt(dmid) and TCNQ molecules is sufficiently strong so as to persist in solution. If such an interaction did not persist in solution and the donor and acceptor molecules were dissociated, only TCNQ would have adsorbed onto the TiO_2 surface and the semiconductor would have exhibited a pale yellow-brown color characteristic of neutral TCNQ. Thus, the presence of the TCNQ molecule in **3** serves two purposes: it causes an increase in molar absorptivity across the visible and into the NIR region, and the peripheral cyano groups serve as anchoring groups to facilitate the adsorption of the adduct onto the surface of the semiconductor. It should be noted that recent 2-D HOESY and PGSE NMR investigations have shown that similar donor−acceptor intermolecular interactions involving trinuclear Au(I) complexes also persist in solution.[24]

The films sensitized by the dye solution of **3** were tested in a "sandwich" solar cell configuration employing an electrolyte that contains 0.6 M dimethylpropylimidazolium iodide, 0.1 M iodine, 0.5 M *tert*-butylpyridine, and 0.1 M lithium iodide in methoxyacetonitrile. The incident photon-to-current conversion efficiency (IPCE) value is ∼0.5% and yields a short circuit photocurrent density of 50 ± 10 μA/cm^2. The open circuit potential is 18 ± 5 mV, and the fill factor was nonmeasurable.

The favorable spectroscopic characteristics and an evaluation of the electrochemical data for the compounds described in this work provide a convenient backdrop for future studies aimed at synthesizing promising candidates for efficient solar cell dyes. The strong continuous absorptions across the visible and into the NIR region observed for the compounds are especially encouraging. There are two major electrochemical requirements for solar cell dyes.[8] One important criterion is for the dye to exhibit a lower first reduction potential (higher energy) than the conduction band of the semiconductor to allow for the injection of an electron from the excited electronic state of the dye into the conduction band of the semiconductor. Second, a higher first oxidation potential (lower energy) than that for the redox electrolyte (usually I^-/I_3^-) is required to allow for the reduction of the oxidized dye molecules back to their electronic ground state. The poor conversion efficiency obtained for the representative dye tested is most likely a consequence of the values of the reduction potentials of **3** ($E_{1/2}$ = −0.33 and 0.19 V; Table 4), which lie at lower energies than that of the conduction band of TiO_2. To remedy this problem, we are pursuing two classes of compounds. The first class consists of Pt(II), Pd(II), and Ni(II) diimine dithiolato compounds without the nitrile acceptors described here but with the conventional anchoring groups (e.g., carboxylate or phosphonate substituents on the bipyridine in **1** and **2**). By inspecting the donor redox potentials in Table 4,[25] one notices that all the reduction potentials are more negative than the ∼−0.6 V value of the conduction band of TiO_2 and that all oxidation potentials are more positive than the ∼+0.2 V value for the I^-/I_3^- redox couple, hence satisfying both electrochemical requirements with a good driving force for each.[26] Adducts of this first class with other organic acceptors that exhibit more suitable negative first reduction potentials[27] will also be studied.

The second class of compounds consists of [M(terpy)X]A salts, where M = Pt(II) or Pd(II), terpy = terpyridine, X = SCN^- or halide, and A is an anion of an organic acceptor

(22) Freed, K. F.; Jortner, J. *J. Chem. Phys.* **1970**, *52*, 6272.
(23) (a) Barbe, Ch. J.; Arendse, F.; Comte, P.; Jirousek, M.; Lenzmann, F.; Shklover, V.; Grätzel, M. *J. Am. Ceram. Soc.* **1997**, *80*, 3157. (b) Burnside, S. D.; Shklover, V.; Barbe, Ch. J.; Comte, P.; Arendse, F.; Brooks, K.; Grätzel, M. *Chem. Mater.* **1998**, *10*, 2419. (c) Nazeeruddin, M. K.; Péchy, P.; Renouard, T.; Zakeeruddin, S. M.; Humphry-Baker, R.; Comte, P.; Liska, P.; Cevey, L.; Costa, E.; Shklover, V.; Spiccia, L.; Deacon, G. B.; Bignozzi, C. A.; Grätzel, M. *J. Am. Chem. Soc.* **2001**, *123*, 1613.
(24) Burini, A.; Fackler, J. P., Jr.; Galassi, R.; Macchioni, A.; Omary, M. A.; Rawashdeh-Omary, M. A.; Pietroni, B. R.; Sabatini, S.; Zuccaccia, C. *J. Am. Chem. Soc.* **2002**, *124*, 4570.
(25) Ni(II) diimine dithiolato complexes are expected to have redox potentials similar to those for their Pt(II) analogues. See: Cocker, T. M.; Bachman, R. E. *Inorg. Chem.* **2001**, *40*, 1550.

(e.g., $TCNQ^{\bullet-}$ $TCNE^{-}$). The first reduction potentials for these anionic complexes will be approximately the same as the second reduction potentials for the corresponding neutral acceptors (i.e., −0.3 to −0.4 V for $TCNQ^{-}$ and ∼−0.8 V for $TCNE^{-}$; Table 4). While only the $TCNE^{-}$ salts can be suitable for TiO_2-based solar cells, the $TCNQ^{-}$ can be used in solar cells based on SnO_2 because this semiconductor has a conduction band that lies ∼0.5 V more positive than TiO_2.[28] On the basis of the results reported in this study, it appears that there is no need for anchoring groups for the second class of compounds, owing to the presence of cyano groups in the organic acceptor anion which allow the dyes to adsorb onto the TiO_2. The result is an increased extinction coefficient in these donor−acceptor salts.

Conclusions

New supramolecular compounds based on 2:1 charge transfer sandwich adducts between diimine dithiolato complexes of Pt(II) and Pd(II) as donors (D) and a variety of organic nitriles as acceptors (A) have been prepared and their structural and optoelectronic properties elucidated. The supramolecular structure consists of −DDADDADDA− stacks with shorter D−D distances than the corresponding values found for crystals of the parent donors. Infrared data suggest a partial negative charge on the TCNQ acceptor units (e.g., ρ ∼−0.4 on the TCNQ unit in **3** and **6**). The impact of the charge distribution upon the formation of the donor−acceptor adducts has been probed by magnetic, conductivity, and spectroscopic studies. The platinum-based charge-transfer compounds exhibit temperature-independent paramagnetism (TIP) with $\chi_{TIP} \sim 10^{-3}$ emu/mol, the magnitude of which is typically associated with Pauli paramagnetism originating from conduction electrons. Also, clear SEM images were obtained for **3**−**5** suggesting that these compounds are not insulators. The conductivities of pressed pellets of **3**, however, are low ($\sim 10^{-6}\ \Omega^{-1}$ at 300 K). Optical and preliminary solar cell studies suggest that the donor−acceptor interactions observed in the solid state also persist in solution. The charge-transfer complexes exhibit appreciable molar absorptivities across the visible and into the near-infrared region, making them potentially useful as solar cell dyes. Preliminary results indicate that solutions of **3** adsorb onto the surface of TiO_2 owing to the presence of the peripheral cyano groups, thus opening up a new avenue for the development of new solar cell dyes that do not possess additional anchoring groups. We are continuing such studies for the use of classes of complexes that are closely related to the compounds described in this paper as dyes for solar cells based on a variety of wide band gap semiconductors, including TiO_2 and SnO_2.

Experimental Section

Starting Materials. All operations were performed under a nitrogen atmosphere using standard Schlenk-line techniques unless otherwise indicated. Solvents were distilled prior to use from the appropriate drying agents. The starting materials K_2PtCl_4 and K_2PdCl_4 were purchased from Pressure Chemical Co. and were reacted with dbbpy[29] to prepare (dbbpy)$PtCl_2$ and (dbbpy)$PdCl_2$ by modifications of a published procedure.[30]

Physical Measurements. IR spectra were measured as Nujol mulls between KBr or CsI plates on a Nicolet 740 FT-IR spectrometer. Electronic absorption spectra were measured at the University of North Texas using a Perkin-Elmer Lambda 900 double-beam UV/vis/NIR spectrophotometer. The solution measurements were carried out for compounds dissolved in HPLC grade CH_2Cl_2, and it was necessary to adjust the concentration and the light path depending on the intensity of the relevant absorption bands desired (e.g., the weak bands in the NIR region required measurements for nearly saturated solutions in a 1 cm quartz cuvette while the strong UV/vis bands required measurements for dilute solutions in a 1 mm quartz cuvette). The solid-state diffuse reflectance spectra were measured using a 150-mm integrating sphere accessory to the Lambda 900 spectrophotometer by either packing the crystalline solid in a 0.1 mm quartz cuvette or preparing a thin film of the solid on a filter paper by adding a few drops of a saturated CH_2Cl_2 solution of the relevant compound at the center of the filter paper and letting the solution evaporate to dryness. Variable-temperature magnetic susceptibility data were obtained in the range of 2−300 K on polycrystalline samples with the use of a Quantum Design model MPMS-XL magnetometer at Texas A&M University. Data were corrected for diamagnetic contributions calculated from Pascal's constants.[31] The cyclic voltammetric studies were performed on a CH Instruments electrochemical analyzer in dichloromethane containing 0.1 M tetra-*n*-butylammonium hexafluorophosphate ([TBA][PF_6]) as the supporting electrolyte. The working electrode was a BAS Pt disk electrode, the reference electrode was Ag/AgCl, and the counter electrode was a Pt wire. The Cp_2Fe/Cp_2Fe^{+} couple occurs at +0.48 V vs Ag/AgCl under the same experimental conditions.

Syntheses. (dbbpy)Pt(dmid), 1. A 40.8 mg (1.96×10^{-4} mol) sample of 1,3,4,6-tetrathiapentalene-2,5-dione was combined with 30 mg (4.4×10^{-4} mol) of NaOEt in 30 mL of MeOH and gently heated for 1 h to give a yellow solution. A suspension of (dbbpy)$PtCl_2$ (106.3 mg, 1.989×10^{-4} mol) in 15 mL of MeOH was added, and the resulting purple product was collected by filtration after 30 min and washed with water, methanol, and diethyl ether. The yield was 95.7 mg (76%). IR (CsI−Nujol; cm^{-1}): 1671 m, 1618 m, 1499 w, 1413 w, 1268 w, 1088 w, 1022 w, 971 w, 939 w, 920 w 897 w, 888 w, 824 w, 591m, 463 w, 366 w, and 316 w. Anal. Calcd for $C_{21}H_{24}N_2OPtS_4$: C, 39.18; H, 3.76; N, 4.35. Found: C, 38.89; H, 3.82; N, 4.09.

(dbbpy)Pd(dmid), 2. A procedure similar to the one used to prepare **1** was followed for the synthesis of **2** (51.4 mg $C_4S_4O_2$, 45

(26) In support of this conclusion, we note that TiO_2-based solar cell studies of similar Pt(II) diimine dithiolate compounds with carboxylate anchoring groups have been reported and exhibited good conversion efficiencies. See: (a) Islam, A.; Sugihara, H.; Hara, Kohjiro; Singh, L. P.; Katoh, R.; Yanagida, M.; Takahashi, Y.; Murata, S.; Arakawa, H.; Fujihashi, G. *Inorg. Chem.* **2001**, *40*, 5371. (b) Islam, A.; Sugihara, H.; Hara, K.; Singh, L. P.; Katoh, R.; Yanagida, M.; Takahashi, Y.; Murata, S.; Arakawa, H. *New J. Chem.* **2000**, *24*, 343.

(27) (a) Loutfy, R. O.; Hsiao, C. K.; Ong, B. S.; Keoshkerian, B. *Can. J. Chem.* **1984**, *62*, 1877. (b) Kaplan, M. L.; Haddon, R. C.; Bramwell, F. B.; Wudl, F.; Marshall, J. H.; Cowan, D. O.; Gronowitz, S. *J. Phys. Chem.* **1980**, *40*, 1550.

(28) For examples of SnO_2-based solar cells, see: (a) Bedja, I.; Hotchandani, S.; Kamat P. V. *J. Phys. Chem.* **1994**, *98*, 4133. (b) Nasr, C.; Hotchandani, S.; Kamat P. V. *J. Phys. Chem. B* **1998**, *102*, 4944. (c) Nasr, C.; Kamat P. V.; Hotchandani, S. *J. Phys. Chem. B* **1998**, *102*, 10047.

(29) Belser, P.; von Zelewsky, A. *Helv. Chim. Acta* **1980**, *63*, 1675.

(30) Juris, A.; Balzani, V.; Barigelletti, F.; Campagna, S.; Belser, P.; von Zelewsky, A. *Coord. Chem. Rev.* **1988**, *84*, 85.

(31) *Theory and Applications of Molecular Paramagnetism*; Boudreaux, E. A., Mulay, L. N., Eds.; John Wiley & Sons: New York, 1976.

mg NaOEt, and 109.6 mg (dbbpy)$PdCl_2$ to yield 78.6 mg (58%) of a wine-red solid). IR (CsI−Nujol; cm^{-1}): 1670 m, 1614 m, 1504 w, 1411 w, 1251 w, 1080 w, 1035 w, 916 w, 897 w, 828 w, 594 m, 468 w, and 344 w. Anal. Calcd for $C_{21}H_{24}N_2OPdS_4$: C, 45.44; H, 4.36; N, 5.05. Found: C, 43.41; H, 5.02; N, 3.96.

[(dbbpy)Pt(dmid)]$_2$[TCNQ], 3. A quantity of TCNQ (10.3 mg) in 20 mL of a 1:1 solution of CH_2Cl_2−benzene was layered with a solution of 65.2 mg of (dbbpy)Pt(dmid) in 10 mL of CH_2Cl_2 (dark purple). After 10 days, the intense blue-purple solution was slowly evaporated and combined with 15 mL of benzene, filtered, and washed with benzene to yield 56.8 mg (75%) of black crystals. IR (CsI−Nujol; cm^{-1}): 2209 m, 1774 w, 1665 m, 1616 m, 1533 m, 1415 w, 1312 w, 1266 w, 1253 w, 1205 w, 1168 w, 1154 w, 971 w, 920 w, 889 w, 833 w, 821 w, 600 w, and 473 w. We have attempted twice to obtain elemental analysis data for the donor−acceptor adducts **3**−**6**, but the results were unsatisfactory. It has been our experience that TCNX materials are problematic for elemental analysis, possibly due to partial decomposition.

[(dbbpy)Pt(dmid)]$_2$[TCNQF$_4$], 4. The method to prepare **3** was used in the synthesis of **4** (111.1 mg of (dbbpy)Pt(dmid) and 24.2 mg of $TCNQF_4$). After 2 weeks, black platelets were harvested, 116.9 mg (86% yield). IR (CsI−Nujol; cm^{-1}): 2210 w, 2190 m, 2168 w, 2143 w, 1768 w, 1667 m, 1617 m, 1574 w, 1522 w, 1418 w, 1340 w, 1253 w, 1202 w, 1172 w, 1133 w, 970 w, 921 w, 900 w, 885 w, 834 w, 660 m, 600 w, and 475 w.

[(dbbpy)Pt(dmid)]$_2$[TCNE], 5. The method used for the preparation of **3** was also used in the synthesis of **5** (0.111 g of (dbbpy)-Pt(dmid) and 11.4 mg of TCNE). A red-brown solution formed after 5 days. After 2 weeks, the resulting black needles were collected by filtration and washed with benzene to give 90 mg (73% yield). IR (CsI−Nujol; cm^{-1}): 2234 w, 2200 m, 2143 w, 1796 w, 1768 w, 1676 m, 1616 m, 1601 m, 1535 w, 1416 w, 1305 w, 1260 m, 1206 w, 1170 w, 1155 w, 1022 w, 917 w, 887 w, 839 w, 803 w, 739 w, 674 m, 617 w, 598 w, 472 w, 400 w, and 369 m.

[(dbbpy)Pd(dmid)]$_2$[TCNQ], 6. A procedure similar to the preparation of **3** was used to prepare **6** (48.8 mg of (dbbpy)Pd-(dmid) and 8.9 mg of TCNQ to afford 26 mg (45%) of black crystals). IR (CsI−Nujol; cm^{-1}): 2212 m, 2143 w, 1657 m, 1612 m, 1534 m, 1412 w, 1314 w, 1266 w, 1252 w, 1204 w, 1175 w, 1154 w, 970 w, 916 w, 834 w, 823 w, 601 w, and 471 w.

X-ray Crystallographic Details and Structure Solution. For compounds **1**−**3** and **5** and **6**, the data were collected on a Bruker-AXS SMART 1000 CCD diffractometer at 110 ± 2 K while for compound **4** the data were collected on a Bruker-AXS SMART APEX CCD diffractometer at 110 ± 2 K with graphite monochromated Mo Kα ($\lambda(\alpha)$ = 0.710 73 Å) radiation. The data were corrected for Lorentz and polarization effects. The Siemens SAINT[32] software package was used to integrate the frames, and the data were corrected for absorption using the SADABS program.[33] The structures were solved by direct methods by the use of the SHELXS-97 program[34] in the Bruker SHELXTL v5.1[35] software package. The SHELXL-97 program[36] was employed to refine all non-hydrogen atoms with anisotropic thermal parameters by full matrix least squares calculations on F^2. Hydrogen atoms were inserted at calculated positions and constrained with isotropic thermal parameters. Crystallographic parameters are listed in Table 1 with any special refinement conditions noted in the following paragraphs.

(dbbpy)Pt(dmid)·CH$_2$Cl$_2$, 1·CH$_2$Cl$_2$. Violet rectangular-shaped crystals were grown by slow evaporation of a CH_2Cl_2 solution of **1** in air.

(dbbpy)Pd(dmid)·C$_6$H$_6$, 2·C$_6$H$_6$. Brown platelets were grown by evaporation of a solution of **2** in a 1:1 ratio of C_6H_6−CH_2Cl_2.

[(dbbpy)Pt(dmid)]$_2$[TCNQ]·2CH$_2$Cl$_2$, 3·2CH$_2$Cl$_2$. Black rectangular-shaped crystals were grown by slow diffusion of a solution of (dbbpy)Pt(dmid) in CH_2Cl_2 with TCNQ in a 1:1 ratio of CH_2Cl_2−C_6H_6 and subsequent evaporation of the resulting solution.

[(dbbpy)Pt(dmid)]$_2$[TCNQF$_4$]·2CH$_2$Cl$_2$, 4·2CH$_2$Cl$_2$. Black platelets were grown by slow diffusion of a solution of (dbbpy)Pt(dmid) in CH_2Cl_2 with $TCNQF_4$ in a 1:1 ratio of CH_2Cl_2−C_6H_6 and subsequent evaporation of the dark solution.

[(dbbpy)Pt(dmid)]$_2$[TCNE]·C$_6$H$_6$, 5·C$_6$H$_6$. Black needles were grown by slow diffusion of a solution of (dbbpy)Pt(dmid) in CH_2Cl_2 with TCNE in a 1:1 ratio of CH_2Cl_2−C_6H_6 and subsequent evaporation of the resulting solution. A disordered benzene molecule was modeled with restraints on atomic distances.

[(dbbpy)Pd(dmid)]$_2$[TCNQ]·2CH$_2$Cl$_2$, 6·2CH$_2$Cl$_2$. Black rectangular crystals were grown by slow diffusion of a solution of (dbbpy)Pd(dmid) in CH_2Cl_2 with TCNQ in a 1:1 ratio of CH_2Cl_2−C_6H_6 and subsequent evaporation of the resulting solution.

Acknowledgment. We are grateful to the Robert A. Welch Foundation for funding of this research to K.R.D. and M.A.O. through Grants A-1449 and B-1542, respectively. M.A.O. thanks the University of North Texas for providing funds to purchase the Lamda-900 UV/vis/NIR spectrophotometer. K.R.D. thanks the National Science Foundation for support of the CCD diffractometer (Grant CHE-9807975) and the SQUID magnetometer (Grant NSF-9974899) as well as a PI grant (CHE-9906583). The authors are grateful to Dr. Md. K. Nazeeruddin for conducting the preliminary TiO_2 solar cell measurements for **3** at the Laboratory for Photonics and Interfaces, Swiss Federal Institute of Technology.

Supporting Information Available: X-ray crystallographic files, in CIF format, for complexes **1**−**6** and further electronic spectral data in the solid state and solution. This material is available free of charge via the Internet at http://pubs.acs.org.

IC0259585

(32) *SAINT, Program for area detector absorption correction*; Siemens Analytical X-ray Instruments Inc.: Madison, WI, 1994−1996.
(33) Sheldrick, G. M. *SADABS, Program for Siemens area detector absorption correction*; University of Gottingen: Gottingen, Germany, 1996.
(34) Sheldrick, G. M. *SHELXS-97. A Program for Crystal Structure Solution*; University of Gottingen: Gottingen, Germany, 1997.
(35) Sheldrick, G. M. *SHELXTL, An integrated system for solving, refining and displaying crystal structures from diffraction data (Revision 5.1)*; University of Gottingen: Gottingen, Germany, 1985.
(36) Sheldrick, G. M. *SHELXL-97. A Program for Crystal Structure Refinement*; University of Gottingen: Germany, 1997.